Journal of Alloys and Compounds 536S (2012) S389–S393

Contents lists available at SciVerse ScienceDirect

Journal of Alloys and Compounds

journal homepage: www.elsevier.com/locate/jallcom

First order reversal curve analysis on NdFeB nanocomposite ribbons subjected to Joule heating treatments

L.G. Pampillo[a], F.D. Saccone[a,*], M. Knobel[b], H.R.M. Sirkin[a]

[a] INTECIN-Instituto de Tecnologías y ciencias de la Ingeniería "Hilario Fernández Long" (UBA-CONICET), Facultad de Ingeniería, Paseo Colón 850 (C1063ACV), C. A. B. A., Argentina
[b] Instituto de Física Gleb Wataghin-Departamento de Física de Materia Condensada-Universidade Estadual de Campinas, Cidade Universitaria Zeferino Vaz, Barao Geraldo 13083-970, Campinas, Sao Paulo, Brazil

ARTICLE INFO

Article history:
Received 29 June 2011
Received in revised form 11 January 2012
Accepted 17 January 2012
Available online 28 January 2012

Keywords:
Composite materials
Nanostructured materials
Rapid-solidification
Magnetic measurements

ABSTRACT

Amorphous precursors with composition $Nd_{4.5}Fe_{72-x}Co_{3+x}Cr_2Al_1B_{17.5}$ ($x = 0$, 2, 7, 12) were thermally treated by the Joule heating technique with a linearly varying electrical current. The crystallization kinetics was followed by monitoring the resistance of the ribbons during the heating up to the final applied current. Crystallized nanostructured phases coexist with an amorphous matrix, as it was observed by means of Mössbauer Spectroscopy and X-ray diffraction.

The irreversible magnetic response of the Joule heated ribbons was analyzed by the First Order Reversal Curves (FORC) diagram technique. For the optimal treatments, associated with the higher maximum energy products for each sample composition, it was found that the main interaction is of a strongly dipolar characteristic. Over annealed samples show a FORC diagram that gives into account of softening, due to grain growth, for those phases precipitated at the first crystallization stage. When it is measured at 20 K, the hardest magnetic sample (Fe = 72 at.%, Co = 3 at.%, I_{final} = 0.5 A), exhibits a diagram with characteristics corresponding to dipolar interactions of soft phases. This fact is consistent with an enhancement of the exchange length due to the increase in the soft phase stiffness as it is expected at low temperatures.

1. Introduction

Since the first KS steel produced in 1916, permanent magnets have been developed continuously as they have found applications in a wide range of devices. Particularly, rare earth magnetic materials have been produced since 1960s. From 1990s, rapid solidification of the Nd–Fe–B ternary alloy became the main route to produce this kind of nanostructured permanent magnets. Among these, Nd-lean nanocomposite magnets are promising candidates due to reduced cost and higher corrosion resistance. Also, they are considered high-performance magnets due to their magnetic properties are higher than the corresponding to the single-phase ones [1]. Then, these exchange-spring magnets exhibit remanence enhancement, moderated to high coercivities and theoretically expected energy products as higher as 8 GJ/m^3 [2]. These properties are due to exchange coupling between hard and soft magnetic phases at nanometric scale. Then, magnetic response is widely dependant on the precipitated phases and the achievement of the optimized nanostructure.

In the Joule heating technique a metallic material is subjected to an electrical current of great intensity for a short time [3]. This allows improving the magnetic properties of ferromagnetic amorphous alloys due to an appropriated nanostructure that can be obtained with a relatively precise control. A variation of this technique, called Linearly Varying Current Joule heating (LVC-JH) [4] consists on the application of an electrical current that varies slowly up to its final value instead of being rapidly set to a fixed intensity. In this way, it is possible to interrupt the annealing runs in certain precise points; which allow us to determine specific annealing parameters in order to obtain optimum properties. This technique is helpful to get information about recrystallization process that occurs after subjecting an amorphous precursor to an electrical current, like those that can be found in fast electrical sintering [5].

First Order Reversal Curve (FORC) diagrams may provide a powerful tool to understand complex aspects in magnetic systems that are not be able to be clarified by means of the hysteresis curves. On a FORC diagram each magnetic system exhibits a characteristic pattern, which contains detailed information about the magnetic properties [6,7]. In the case of Nd-lean permanent magnets, FORC diagrams become also a highly useful tool for the optimized design of electrical machines, despite its lower performance than ultra grade sintered magnets.

* Corresponding author. Tel.: +54 11 4343 0893; fax: +54 11 4331 1852.
E-mail address: fsaccone@fi.uba.ar (F.D. Saccone).

0925-8388/$ – see front matter © 2012 Elsevier B.V. All rights reserved.
doi:10.1016/j.jallcom.2012.01.104

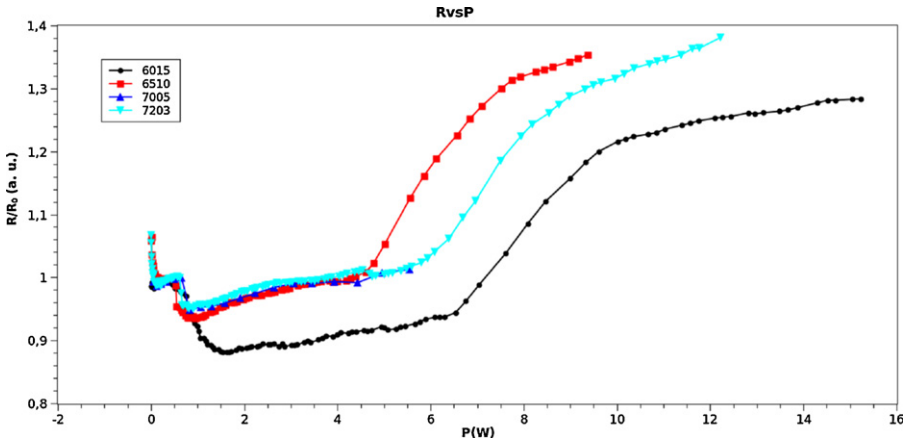

Fig. 1. Resistance (R) vs power (P) curves for samples of the different compositions investigated in this work. In each case, the resistance value is normalized to its corresponding initial value (R_0).

The aim of this paper is to induce by fast heating certain nanostructures in the above mentioned Nd-lean ternary alloy that cause their magnetic hardening and analyze the irreversible switching of magnetization in the ribbons by the FORC diagram technique, in order to correlate the role of selected additive, the corresponding nanostructure and their magnetic responses.

2. Materials and methods

Ingot alloys with nominal composition $Nd_{4.5}Fe_{72-x}Co_{3+x}Cr_2Al_1B_{17.5}$ (x = 0, 2, 7, 12) were prepared by induction melting in Ar atmosphere, starting from elements with 99.995% purity. Amorphous ribbons were produced by quenching the alloys onto a rotating copper wheel with a tangential velocity of 45 m/s. Ribbons typical sizes were 1 mm wide and 20 μm thick.

The ribbons were subsequently treated by Joule heating, using a variation of the technique called linearly varying current Joule heating (LVC-JH). The experimental set up consists of two pairs of U-shaped electrical contacts used to clamp the end of the sample minimizing the contact area. The sample was connected in series to a standard resistance (R = 1 mΩ). The current was varied between 0 to I_{final} at a rate of 0.017 A/s. The experiment was performed in a vacuum atmosphere in order to prevent oxidation.

Amorphous and crystalline ribbons were structurally characterized by means of X-ray diffraction (XRD) in a θ–2θ diffractometer (Rigaku D/max equipped with an horizontal goniometer) using Cu-Kα radiation and by Mössbauer effect spectroscopy (ME) under transmission geometry with a standard constant acceleration spectrometer using a 10 mCi ^{57}CoRh radioactive source. The isomer shifts δ were referred to RT α-Fe. For fitting the Mössbauer spectra were employed the hyperfine fields corresponding to the majority phases that were clearly identified in a complementary way by XRD. At intermediate stages of crystallization we discarded the six iron sites of the $Nd_2Fe_{14}B$ phase (Φ-phase) due to their interferences with the distribution of hyperfine fields of the amorphous phase. Due to the low content of this phase, an error less than 5% can be expected with this selected criterion.

DC magnetic characterization and FORC experiments were performed at room temperature in a VSM Lakeshore 7280. A FORC measurement begins by saturating the sample with a large positive applied field, after which it is decreased to a reversal field named H_a. The FORC is the curve that starts at H_a and proceeds back to positive saturation. A set of FORCs allows obtaining the FORC distribution, which is the contour plot of a two-dimensional distribution function which is defined as:

$$f(H_a, H_b) = -\frac{1}{2}\frac{\partial^2 M(H_a, H_b)}{\partial H_a \partial H_b} \quad (1)$$

where $M(H_a,H_b)$ is the magnetization of the sample at applied field H_b on the FORC with reversal field H_a, this is well defined only for $H_b > H_a$. FORC distributions were calculated from the experimental curves by a finite differences program. When FORC distribution is plotted, in another common usage their coordinates are transformed to: $H_C = (H_b - H_a)/2$ and $H_U = (H_b + H_a)/2$.

For this last description, the main axes are rotated 45° and $H_C = 0$ corresponds to reversible interactions while $H_U = 0$ indicate a null local mean field at the particle position [8]. On the other hand, any vertical line at H_a–H_b plane corresponds to $H_U = -H_C$ and it can be interpreted as a distribution with a demagnetizing local mean field (as it will be expected for systems where their particles are subjected to dipolar interactions).

From here on, the samples will be denoted as XXYY, with XX = at.% Fe and YY = at.% Co. For instance, the sample 6510 refers to a ribbon with 65 at.% of Fe and 10 at.% of Co.

3. Results and discussion

The LVC-JH treatment is computer controlled, so it is possible the on-line analysis of $R(I)$ curves and, therefore, to precisely determine a current value to interrupt the annealing (I_{final}). Fig. 1 shows $R(P)$ curves, where P stands for the Joule power (I^2R). All the samples investigated in this work showed the same qualitative behaviour. This is, firstly a fast resistance reduction mainly attributable to changes in the contact resistance by removal of surface oxide layers followed by residual stress relaxation. A new resistance drop indicates the beginning of crystallization corresponding to the intermediate metastable phases. After this, follows a gradual increase in the resistance originated in nucleation, diffusion and grain growth that finalizes in a sharply resistance enhancement indicating the starting of secondary crystallization.

As it can be observed from the corresponding XRD results (see Fig. 2) and also confirmed by ME, all the entire process corresponds to an irreversible transformation, including the nearly linear variation observed at the middle power range. As it is shown in the XRD patterns of the 6015 sample (Fig. 2), with I_{final} = 0.4 A (corresponding to 1 W in $R(P)$) there is a high amorphous remnant. Higher applied currents promote an increase in the amount of

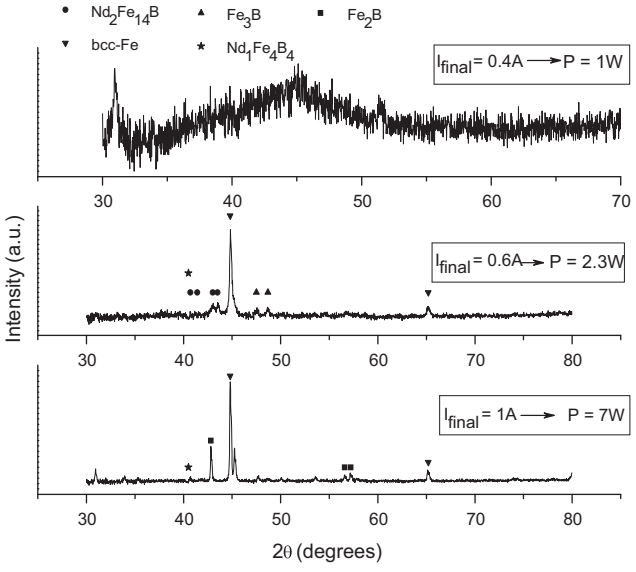

Fig. 2. XRD patterns for 6015 sample treated until different I_{final} values (from top to bottom, they correspond to P = 1 W, 2.3 W and 7 W).

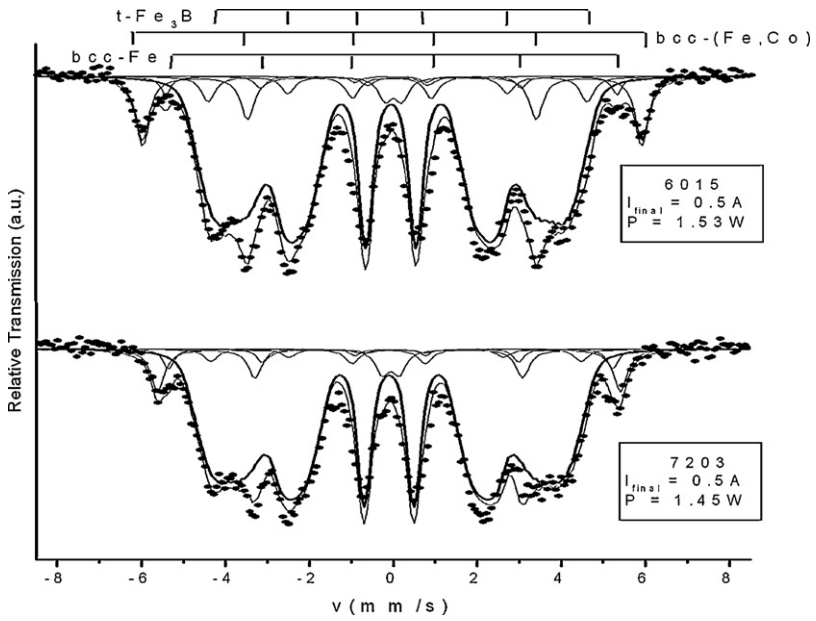

Fig. 3. Mössbauer spectra for 7203 and 6015 samples treated until indicated I_{final} and P values. Marked line corresponds to the distribution of hyperfine fields of the amorphous remnant phase.

crystalline phases and fully (secondary) crystallization was observed for $I_{final} = 1$ A (7 W). Mössbauer spectra of all the samples that showed high coercivities for each composition confirmed that an evolution of crystallization in the middle range of power occurred, rather than a linear trend of resistance originated in a metallic thermal dependence (TCR). Fig. 3 shows the ME spectra of 6015 and 7203, both annealed up to the I_{final} values which correspond to the highest coercivity for each ones. In accordance with $R(P)$ curve description, XRD and ME measurements revealed that ribbons annealed until low I_{final} values have a great remnant amorphous phase (see Figs. 2 and 3). On the other hand, it was detected, by ME, the partial dilution of Co atoms in the bcc-Fe structure. This fact, can be concluded by the presence of a magnetic sextet ($B_{hf} \sim 35T$) which has different relative proportions with the corresponding to bcc-Fe ($33T$), depending on the composition.

At the beginning of crystallization the Joule heated samples show the nucleation of a minority hard magnetic phase (Φ-phase), bcc-Fe and t-Fe_3B. At intermediate applied currents, the best magnetic properties were found beside the great amount of remnant amorphous phase. Table 1 enumerates the magnetic properties of these samples. Room temperature hysteresis loops for the samples corresponding to the discussion of Fig. 3 are shown in Fig. 4.

Table 1
Magnetic properties of each composition sample with optimal response.

Sample/I_{final} (A)–P (W)	H_C (Oe)	$\mu_0 M_S$ (T)	M_R/M_S	BH_{MAX} (MGOe)
7203/0.50–1.45	2660	1.37	0.695	9
7005/0.55–1.6	2640	1.25	0.690	7.9
6510/0.45–1.7	2620	1.38	0.660	8.3
6015/0.50–1.53	2475	1.28	0.750	10.3

Following the magnetic behaviour by FORC diagrams for the optimized treated samples listed in Table 1, at a first glance, they look as having nearly similar characteristics. For both samples, we confirmed the existence of an interaction region of both phases, being the interaction present as a biasing field for the soft phase and a coercivity reduction for the hard one [9]. However, as it can be seen in Fig. 5, for samples that we found as having the highest (7203/0.5 A–1.45 W) and the lowest (6015/0.5 A–1.53 W) coercivities, the diagrams show a significant difference: 6015 exhibits a higher maximum near to origin of $H_C - H_U$ plane (follow from $H_a = 0$ with a perpendicular line intersecting the 45° limit of the diagram) when heated up to 0.5 A–1.53 W (see Fig. 5, left). This fact explains the best squareness and highest BH_{MAX} that shows its hysteresis loop ($M_R/M_S = 0.75$ and 10.3 MGOe, respectively). In fact,

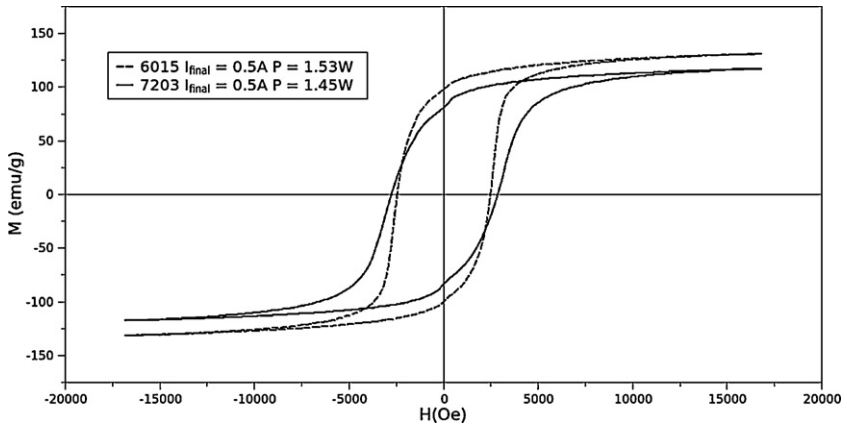

Fig. 4. RT hysteresis loops, corresponding to the samples 7203 and 6015 treated until indicated I_{final} and P values.

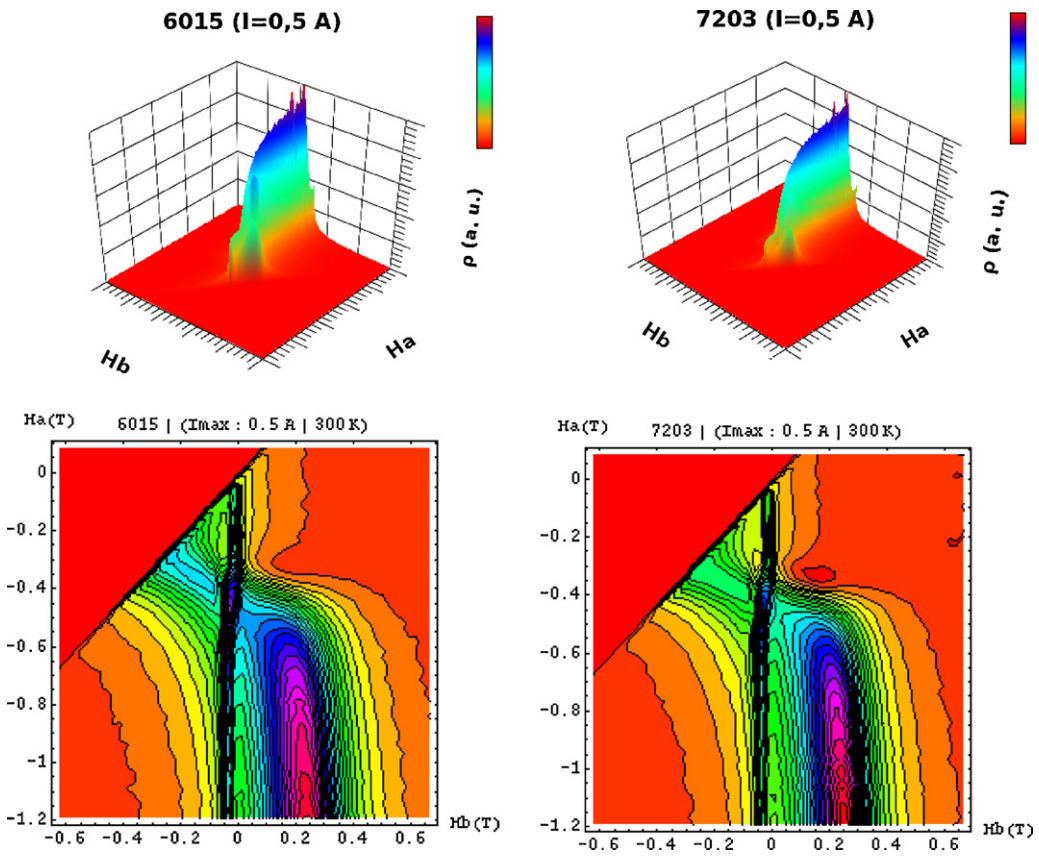

Fig. 5. 2D and 3D FORC diagrams for samples: 6015 (left) and 7203 (right), both treated until I_{final} = 0.5 A (P = 1.53 W and 1.45 W, respectively).

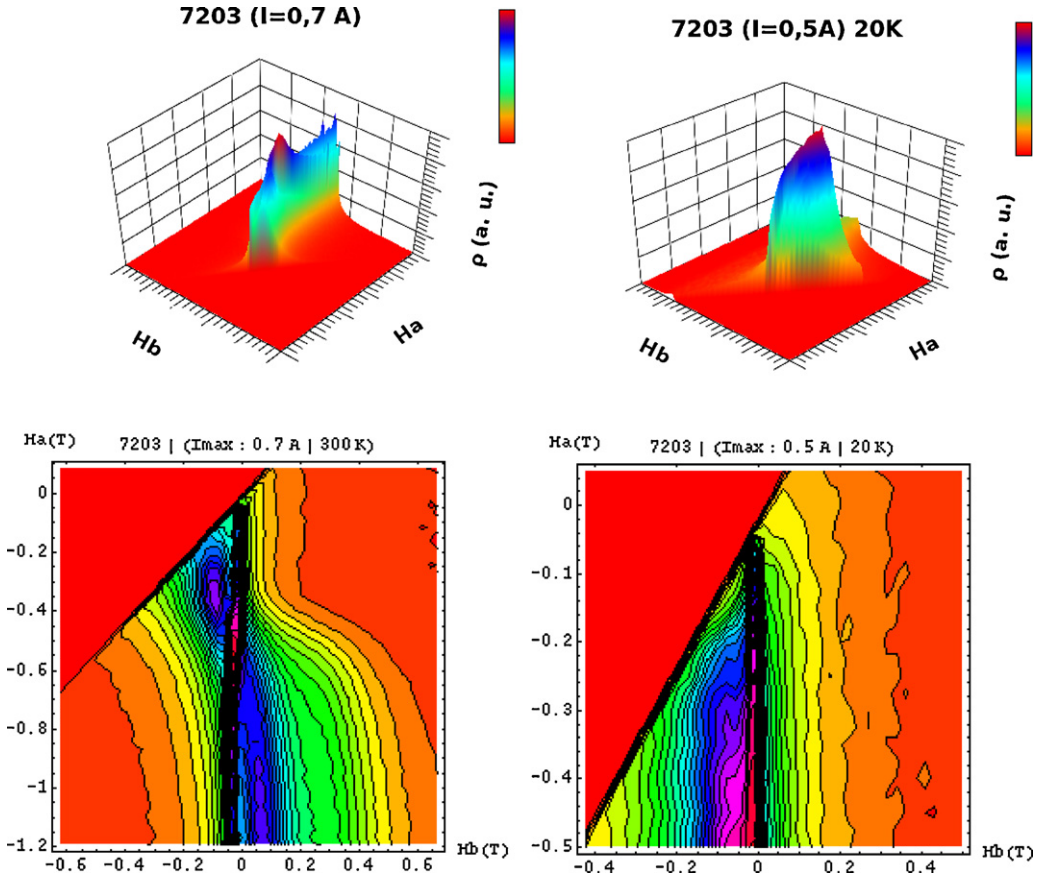

Fig. 6. 2D and 3D FORC diagrams for sample 7203: treated until I_{final} = 0.7 A (P = 3 W, left) and treated until. I_{final} = 0.5 A (P = 1.45 W) and measured at 20 K (right).

remanence enhancement occurs for appropriated relative fractions of well coupled hard and soft phases in ferromagnetic materials [10]. Likewise, we can also observe that the maximum corresponding to 6015 sample is broader than 7203. This is an indication that the switching fields are extended longer.

Higher final currents promote the magnetic softening of the samples as it can be observed from the FORC diagram corresponding to sample 7203 treated until I_{final} = 0.7 A (2.95 W), with its maximum near to 1500 Oe (see Fig. 6, left). The sample with the highest coercive field (7203/0.5 A–1.45 W) also shows a FORC diagram characteristics of a soft magnetic material when it is measured at 20 K (see Fig. 6, right). The exchange length governs the interaction range between soft phases. This is mediated by the hard grains precipitated at the remnant amorphous matrix in the ribbons. The average exchange length [11] can be approximated as it is indicated in Eq. (2). At low temperature, stiffness in the soft matrix is increased in a more intense way than the hard phase anisotropy does. By this way, the coercive field falls for low temperature.

$$L_{ex} = \sqrt{\frac{A_{soft}}{K_{hard}}} \quad (2)$$

4. Conclusions

Joule heating of $Nd_{4.5}Fe_{72-x}Co_{3+x}Cr_2Al_1B_{17.5}$ (x = 0, 2, 7, 12) promoted crystallization of a hard magnetic phase in amorphous precursors produced by melt-spinning. Selection of the maximum applied current in the LVC-JH technique allowed us to analyze the structure and magnetic response of the materials. We found that beside the remnant amorphous matrix a magnetic hardening is present, originated in the precipitation of the hard magnetic phase at the first stage of crystallization. From their FORC diagrams, we detected a maximum for the distribution corresponding to hard and soft magnetic components that are exchange coupled between them. The distribution is elongated along a line that is parallel to the vertical axis of H_a–H_b plane, which gives an idea of a dipolar character in the interactions. Over annealed samples have FORC diagrams with this maximum shifted to the left in concordance with a lowering in the coercive field of their hysteresis loops. Low temperature measurements promoted a magnetic softening of the sample, corresponding to an increase in stiffness of soft phases and amorphous matrix.

For the set of final currents applied in this work, we determined that the sample $Nd_{4.5}Fe_{60}Co_{15}Cr_2Al_1B_{17.5}$ treated at I_{final} = 0.5 A (1.53 W), corresponds to the best magnetic properties, with BH_{MAX} = 10.3 MGOe, H_C = 2475 Oe and a M_R/M_S = 0.750.

Acknowledgements

The authors are grateful to CAPES-SPU cooperation research project "*Propriedades magnéticas e de transporte de sistemas nanoestruturados*" and Conicet (Argentina) for partial support of this work.

References

[1] S. Sugimoto, J. Phys. D: Appl. Phys. 44 (2011) 064001.
[2] E. Kneller, R. Hawig, IEEE Trans. Magn. 27 (1991) 3588–3600.
[3] P. Allia, M. Baricco, P. Tiberto, F. Vinai, Phys. Rev. B 47 (1993) 3118–3125.
[4] F.C.S. ad Silva, E.F. Ferrari, M. Knobble, J. Appl. Phys. 84 (1998) 5366–5368.
[5] T. Saito, H. Ishikawa, D. Nishio-Hamane, J. Appl. Phys. 109 (2011) 07A754.
[6] C.R. Pike, A.P. Roberts, K.L. Verosub, J. Appl. Phys. 85 (1999) 6660–6667.
[7] C.R. Pike, C.A. Ross, R.T. Scalettar, G. Zimanyi, Phys. Rev. B 71 (2005) 134407.
[8] F.D. Saccone, L.G. Pampillo, M.I. Oliva, P.G. Bercoff, H.R. Bertorello, H.R.M. Sirkin, Phys. B 398 (2007) 313.
[9] I. Panagiotopoulos, J. Magn. Magn. Mater. 323 (2011) 2148.
[10] I. Betancourt, H.A. Davies, Mater. Sci. Technol. 26 (2010) 5.
[11] A. Hernando, J. Phys.: Condens. Matter 11 (1999) 9455.